INSTITUTE OF PHYSICS PUBLISHING JOURNAL OF PHYSICS: CONDENSED MATTER

J. Phys.: Condens. Matter **14** (2002) L583–L589 PII: S0953-8984(02)38922-7

LETTER TO THE EDITOR

High-pressure Raman study of CaV_2O_5

Z V Popović[1,4], V Stergiou[2], Y S Raptis[2], M J Konstantinović[1], M Isobe[3], Y Ueda[3] and V V Moshchalkov[1]

[1] Laboratorium voor Vaste-Stoffysica en Magnetisme, Katholieke Universiteit Leuven, Celestijnenlaan 200D, B-3001 Leuven, Belgium
[2] Physics Department, National Technical University of Athens, GR 157 80 Athens, Greece
[3] Institute for Solid State Physics, The University of Tokyo, 5-1-5 Kashiwanoha, Kashiwa, Chiba 277-8581, Japan

Received 7 July 2002
Published 2 August 2002
Online at stacks.iop.org/JPhysCM/14/L583

Abstract

The phonon dynamics of the spin ladder calcium vanadium oxide is studied using Raman spectroscopy under high pressure up to 13.5 GPa. Twelve Raman modes, which are observed and assigned at low pressures, disappear at around 9 GPa. With further pressure increase, three broad modes appear at about 325, 750 and 810 cm^{-1}, indicating the transition of the layered structure into the disordered phase. No scattering activity is found above 13 GPa. The comparison between the vibrational properties of CaV_2O_5, α'-NaV_2O_5 and V_2O_5 indicates that anomalous 448 cm^{-1} mode hardening in α'-NaV_2O_5 under pressure is also due to structural changes. The intercalation of Ca atoms results in a higher compressibility and stability of the CaV_2O_5 crystal structure in comparison with V_2O_5.

The vanadate oxides, AV_2O_5 (A = Li, Na, Cs, Mg and Ca), have demonstrated a variety of the low-dimensional quantum spin phenomena, such as one-dimensional antiferromagnetism in α'-NaV_2O_5 [1] and LiV_2O_5 [2], the antiferromagnetic two-leg ladder structure in CaV_2O_5 [3] and MgV_2O_5 [2], and the spin-dimer structure in CsV_2O_5 [4]. Among all vanadates, α'-NaV_2O_5 has attracted much attention in recent years because of the spin-Peierls-like behaviour of its magnetic susceptibility below the transition temperature of 35 K [1]. It has been found that the phase transition is accompanied both by the lattice distortions and a charge ordering.

The calcium vanadate is isostructural with α'-NaV_2O_5. It has an orthorhombic structure [5] with centrosymmetric space group *Pmmn* and two formula units per unit cell ($Z = 2$). Each V atom is surrounded by five oxygen atoms, forming VO_5 pyramids. These pyramids are mutually connected via common edges to form layers in the (*ab*)-plane. The Ca atoms are situated between these layers as intercalants. Despite having the same crystal structures, the electronic properties of CaV_2O_5 and α'-NaV_2O_5 are quite different. In CaV_2O_5, all vanadium

[4] Permanent address: Institute of Physics-Belgrade, PO Box 68, 11080 Belgrade/Zemun, Yugoslavia.

ions are in the V^{4+} oxidation state and have $S = 1/2$. α'-NaV_2O_5 is a mixed-valence compound (V^{4+}:V^{5+}= 1:1) with valence electrons attached to the V–O–V molecular orbital of the ladder rung.

The effect of pressure on the structural, vibrational and electronic properties of α'-NaV_2O_5 has been discussed in [6–11]. It has been found that the 448 cm^{-1} Raman active mode is particularly sensitive to the structural changes induced by pressure. This mode strongly couples with the electronic continuum and corresponds to the bond bending V–O_3–V vibration. Another important effect is the softening of the V–O_1 Raman active stretching mode under pressure, which appears due to the increased influence of the inter-layer coupling. This observation is not in accordance with x-ray data, which show a shortening of the V–O_1 distance under pressure [7]. Thus, a study of the phonon dynamics in isostructural CaV_2O_5 under pressure, where coupling between phonons and the electronic background is not present, can provide further insight and additional information for the understanding of lattice dynamics in α'-NaV_2O_5 under pressure.

In this letter, we present Raman spectra of CaV_2O_5 polycrystalline samples under pressure. We have found that all Raman lines observed at low pressures disappear at about 9 GPa. Further pressure increase induces three broad bands at about 325, 750 and 810 cm^{-1}, which clearly indicate a phase transition. No scattering activity is found above 13 GPa. We also discuss the pressure dependences of the highest frequency modes of CaV_2O_5 through comparison with the corresponding modes in α'-NaV_2O_5 and V_2O_5.

High-pressure Raman scattering measurements were carried out at room temperature, using a gasketed diamond anvil cell (DAC) [12]. The powder samples were loaded into the cell, with a 4:1 methanol/ethanol mixture as a pressure medium. The details of the sample preparation have been published elsewhere [3]. The standard ruby luminescence was used for pressure calibration. Ar-ion lasers were used as the excitation source. The scattered light was dispersed with a Spex 1403 double monochromator and detected with a conventional photon counting system.

The unpolarized Raman spectra of CaV_2O_5 at ambient ($p = 0.1$ MPa) and high pressures are presented in figure 1. The effect of pressure on the mode frequencies is illustrated in figure 2. The lines show a polynomial ($\omega = A + B_1 p + B_2 p^2$) fit. The best fit parameters are given in table 1. By comparing the ratio of B_2 over B_1 for different modes, we observe (see table 1) that for the highest frequency mode at 932 cm^{-1}, as well as for the 470 cm^{-1} mode, this ratio takes a significantly higher value than the corresponding ratio of all other modes having this ratio as a negative value. The frequencies of all other modes move to higher energies with pressure, without any peculiarity such as crossing, anti-crossing, overlapping or intensity exchange. This result suggests that almost all lattice parameters decrease with increasing pressure while maintaining the same inter-layer and intra-layer symmetry.

The assignment of the observed Raman active modes given in figure 2 is done by comparing mode intensities for parallel and crossed polarized configurations [13, 14] with fully polarized spectra of α'-NaV_2O_5 [15]. Despite the same crystal structure of CaV_2O_5 and α'-NaV_2O_5 there is a remarkable difference in frequencies for some analogous phonon modes, mostly due to the difference in interatomic distances, and the electronic structure. The highest frequency A_{1g} phonon mode appears at 932 cm^{-1} in CaV_2O_5 Raman spectra. This mode represents the V–O_1 bond stretching vibration, see inset in figure 3(a). The larger V–O_1 distance in CaV_2O_5 (1.645 Å, [5]), in comparison with the corresponding interatomic distance in α'-NaV_2O_5 (1.61 Å [16]), causes the frequency shift of this phonon to lower energies. The same conclusion can be made for the highest frequency CaV_2O_5 mode with B_{1g} symmetry at 636 cm^{-1}. This mode originates from the bond stretching vibrations of the V and the O_2 ions along the $\boldsymbol{b}$-axis, see inset in figure 3(d). The next A_{1g} mode of CaV_2O_5 appears at the frequency of 539 cm^{-1} which is close to the frequency of the analogous mode in α'-NaV_2O_5 (534 cm^{-1}).

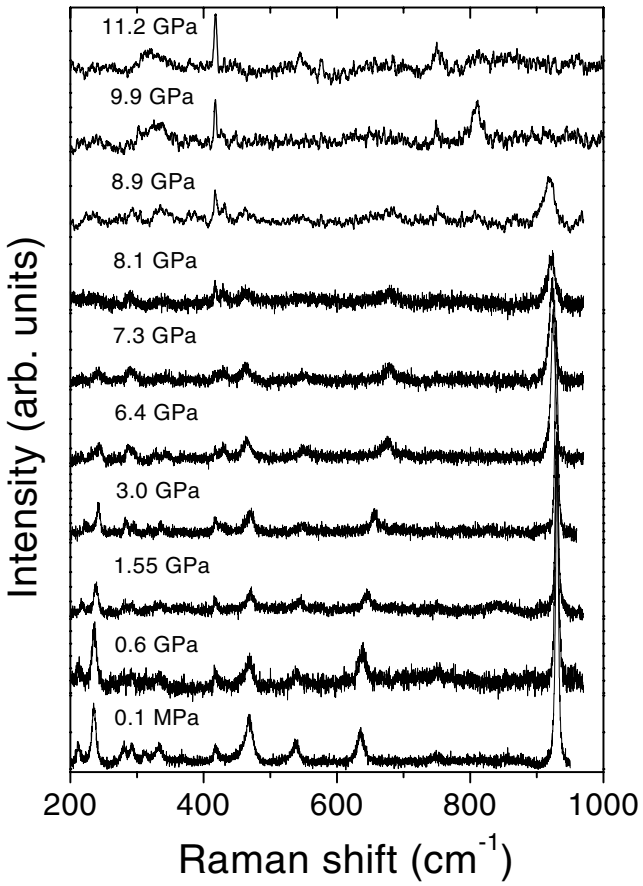

Figure 1. Unpolarized Raman spectra of CaV_2O_5 at room temperature and different pressures.

Table 1. Frequencies and pressure coefficients of Raman active modes of CaV_2O_5. ω represents the mode frequencies at ambient conditions. B_1, B_2 and A are the linear, quadratic and free terms of the polynomial fit $\omega = A + B_1 p + B_2 p^2$, respectively.

ω (cm^{-1})	A (cm^{-1})	B_1 (cm^{-1} GPa^{-1})	B_1/A (10^{-2} GPa^{-1})	B_2 (cm^{-1} GPa^{-2})	B_2/B_1 (1 GPa^{-1})
90	90.3	0.18	0.2	0.214	1.19
212	211	5.48	2.6	−0.284	−0.052
236	235	3.0	1.28	−0.265	−0.088
281	280	0.63	0.22	0.0725	0.115
293	291	1.77	0.61	−0.142	−0.080
310	311	1.946	0.626	0.001	0.051
335	332	1.94	0.584	−0.0614	−0.031
418	417.5	0.59	0.14	0.0967	0.16
470	468	0.856	0.183	−0.181	−0.21
539	537	4.465	0.83	−0.37	−0.083
636	634	9.02	1.425	−0.386	−0.043
932	931	0.165	0.018	−0.147	−0.89

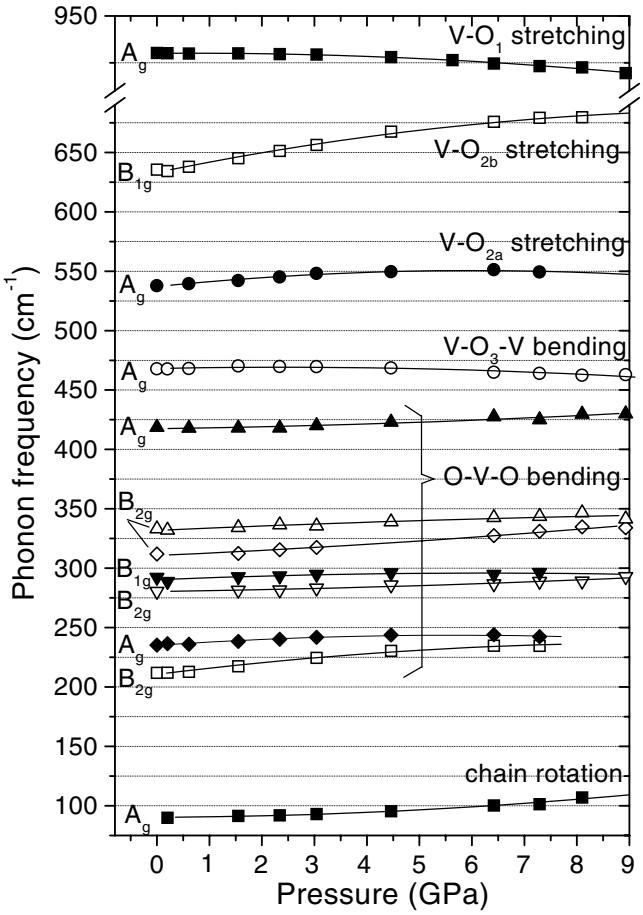

Figure 2. Pressure dependence of Raman mode frequencies of CaV_2O_5. The solid curves are polynomial fits obtained with parameters given in table 1.

This mode represents the bond stretching vibration of V and O_{2a} ions, see inset in figure 3(b). The lack of any noticeable frequency difference between these modes is in accordance with a similar value of the V–O_{2a} bond length in CaV_2O_5 (1.982 Å) and α'-NaV_2O_5 (1.985 Å).

According to the crystallographic data, the V–O_3–V bond bending mode of CaV_2O_5 at 470 cm^{-1} (mainly O_3 ion vibrations along the *c*-axis, see inset in figure 3(c)) should appear at a frequency lower than the frequency of the analogous mode in α'-NaV_2O_5 (448 cm^{-1}), because the V–O_3–V bond length in CaV_2O_5 (3.81 Å) is larger than that of α'-NaV_2O_5 (3.64 Å). This apparent discrepancy is easy to understand if we bear in mind that the renormalized frequency (no electron–phonon interaction) of the V–O_3–V bond bending mode in α'-NaV_2O_5 (V_2O_5) is at 485 cm^{-1} [15] (483 cm^{-1} [17]).

In figure 3 we compare the pressure-induced frequency shifts of the four highest frequency modes in CaV_2O_5, α'-NaV_2O_5 and V_2O_5. Besides similarities in the crystal structure (all of them have the same layered structure built from the edge sharing VO_5 square pyramids) these compounds differ with respect to the formal oxidation state of the V ions, which is 4+ in CaV_2O_5, 4.5+ in α'-NaV_2O_5 and 5+ in V_2O_5. As can be seen in figure 3, the highest frequency modes of the A_{1g} (figure 3(a)) and the B_{1g} (figure 3(d)) symmetries have the same kind of mode

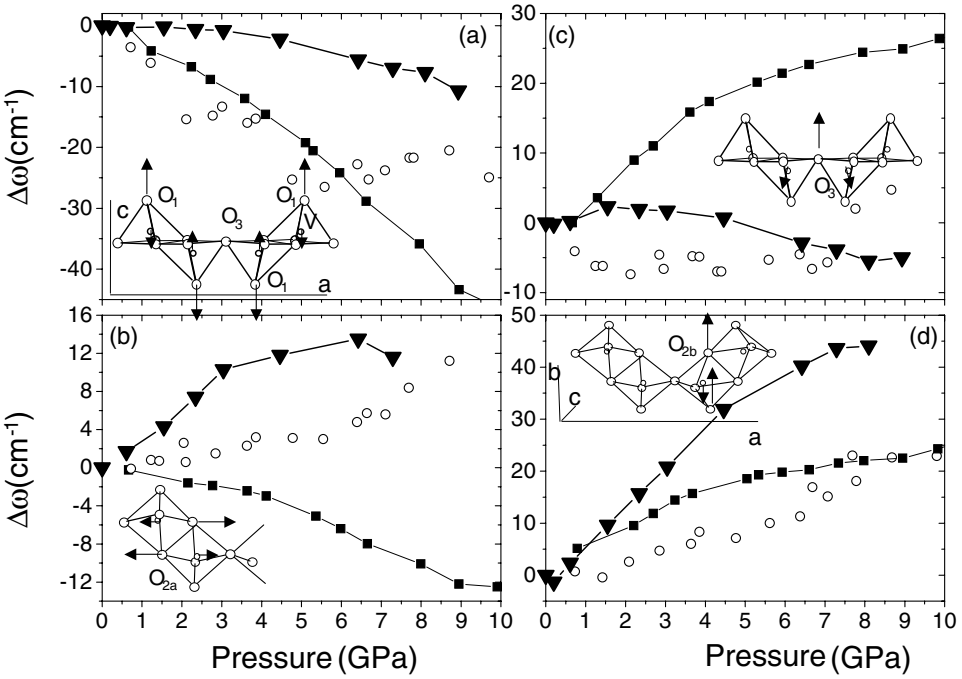

Figure 3. Pressure frequency shift of several Raman modes of CaV_2O_5 (▼) in comparison with the corresponding modes of α'-NaV_2O_5 (■) and V_2O_5 (○). The insets show the ion displacement patterns of the corresponding modes: (a) the V–O_1 bond stretching A_{1g} symmetry mode at 969 cm^{-1} (α'-NaV_2O_5), 932 cm^{-1} (CaV_2O_5), 997 cm^{-1} (V_2O_5); (b) the V–O_{2a} bond stretching A_{1g} symmetry mode at 534 cm^{-1} (α'-NaV_2O_5), 539 cm^{-1} (CaV_2O_5), 524 cm^{-1} (V_2O_5); (c) the V–O_3–V bond bending A_{1g} symmetry mode at 448 cm^{-1} (α'-NaV_2O_5), 470 cm^{-1} (CaV_2O_5), 478 cm^{-1} (V_2O_5); (d) the V–O_{2b} bond stretching B_{1g} symmetry mode at 684 cm^{-1} (α'-NaV_2O_5), 636 cm^{-1} (CaV_2O_5), and 702 cm^{-1} (V_2O_5).

frequency versus pressure dependence in all three compounds. The A_{1g} modes at 539 cm^{-1} (figure 3(b)) and 470 cm^{-1} (figure 3(c)) have opposite frequency versus pressure dependence in α'-NaV_2O_5 and in CaV_2O_5 (V_2O_5).

The V–O_1 bond stretching mode (see figure 3(a)) softens with increasing pressure in all three compounds. The softening is much stronger in α'-NaV_2O_5 (50 cm^{-1} at $p = 10$ GPa) and V_2O_5 (25 cm^{-1} at $p = 6$ GPa [18]) than in CaV_2O_5 (11 cm^{-1} at $p = 9$ GPa). The strong softening of the V–O_1 stretching mode in α'-NaV_2O_5 and V_2O_5 is due to the increase influence of the inter-layer V$\cdots$$O_1$ bond under pressure, which leads to a continuous change in the V coordination from square pyramidal towards octahedral [9, 10, 18]. In the case of CaV_2O_5, due to the larger Ca ion radius, the inter-layer interaction is reduced, and softening is considerably smaller.

The pressure-induced frequency shift of the V–O_{2a} bond stretching mode at 539 cm^{-1} in CaV_2O_5 is positive (see figure 3(b)) and somewhat stronger than in V_2O_5. The negative frequency shift of the corresponding mode in α'-NaV_2O_5 is, most probably, a consequence of coupling between this mode and the electronic background peaked at about 650 cm^{-1}. This type of electronic background is not presented either in CaV_2O_5 or in V_2O_5.

The most intriguing pressure dependence is observed for the V–O_3–V bond bending vibration. This mode hardens by 25 cm^{-1} in α'-NaV_2O_5 when the pressure is increased

to 10 GPa [9]. The corresponding modes in CaV_2O_5 and V_2O_5 show (figure 3(c)) a very small frequency shift under pressure. Such a large difference between Na and Ca vanadate pressure dependences for this mode can be due to change in the electronic structure, and/or due to the structural changes.

According to the V–O_3–V bond length in these three compounds (3.81 Å in CaV_2O_5, 3.64 Å in α'-NaV_2O_5, 3.56 Å in V_2O_5 [17]), the V–O_3–V bond bending vibration in α'-NaV_2O_5 should have an energy higher than in CaV_2O_5 and smaller than in V_2O_5. However, the presence of a single electron in the V–O_3–V rung of α'-NaV_2O_5 strongly affects the bond bending force constant and shifts the energy to 448 cm^{-1}. As a consequence, the charge ordering transition ($T_c = 34$ K) is expected to have fingerprints in the energy versus temperature behaviour of this mode, which is not observed. Such an intriguing dissonance is similar to the observed mode behaviour under pressure, thus indicating that simple structural changes may be behind these findings. Indeed, the V–O_3–V bond length in α'-NaV_2O_5 decreases from 3.64 Å at ambient pressure to 3.56 Å (3.52 Å) at 5.4 GPa (15.5 GPa) [7]. We make an approximate estimation for the change of the bond bending force constant by scaling the frequency as the square root of the force constant, and assuming a scaling of the force constants as R^{-6} (R is the bond length). Similarly, scaling of the phonon frequency for the bond stretching mode is R^{-3}. In our case, R (O–V_3–O)$_0$/R(O–V_3–O)$_{5.6\,GPa}$ is 1.0225. This parameter can produce an increase of the phonon frequency of about 7% (about 30 cm^{-1} in the case of $\omega = 448$ cm^{-1}), which is enough to explain the observed phonon frequency shift of the V–O_3–V bond bending mode under pressure.

Finally, in figure 3(d) we compare the frequency versus pressure dependences of the V–O_{2b} bond stretching mode. This mode represents the out-of-phase bond stretching vibration of the B_{1g} symmetry. The large frequency shift of this mode under pressure in CaV_2O_5 is related to a larger compressibility along the ***b***-axis in CaV_2O_5 (the V–O_{2b} distance in CaV_2O_5 is about 2% larger than in α'-NaV_2O_5).

Let us refer back to figure 1. A dramatic spectral change occurs above 9 GPa, where the strongest peak of CaV_2O_5 at 932 cm^{-1} also disappears. At the same pressure (10 GPa) three broad modes appear at ∼325, 750 and 810 cm^{-1}. At a pressure of 11.2 GPa the mode at about 750 cm^{-1} becomes more intense than the 810 cm^{-1} mode and a broad structure at about 650 cm^{-1} starts to develop. The shape and frequency of these modes correspond to those of amorphous $NaVO_3$ [19]. This means that the pressure of 10 GPa causes complete breakdown of the CaV_2O_5 crystal structure, keeping short-range ordering up to 13 GPa.

In conclusion, we have studied the Raman scattering in spin ladder calcium vanadium oxide under high pressure up to 13.5 GPa. Twelve modes, which are observed and assigned at low pressures, disappear at around 9 GPa. With further pressure increase, three broad modes appear at about 325, 750 and 810 cm^{-1}, indicating the transition of the layered structure of CaV_2O_5 into a disordered phase. No scattering activity is found above 13 GPa. Finally, a comparison between the pressure dependence of four distinctive modes of CaV_2O_5, α'-NaV_2O_5 and V_2O_5 is presented in terms of their crystallographic as well as V-oxidation states.

This work was supported by the Serbian Ministry of Science and Technology, by the National Technical University, Athens, and by the GOA and FWO projects at K U Leuven.

References

[1] Isobe M and Ueda Y 1996 *J. Phys. Soc. Japan* **65** 1178
[2] Isobe M, Ueda Y, Takizawa K and Goto T 1998 *J. Phys. Soc. Japan* **67** 755

[3] Iwase H, Isobe M, Ueda Y and Yasuoka H 1996 *J. Phys. Soc. Japan* **65** 2397
[4] Isobe M and Ueda Y 1996 *J. Phys. Soc. Japan* **65** 3142
[5] Onoda M and Nishiguchi N 1996 *J. Solid State Chem.* **127** 359
[6] Nakao H, Ohwada K, Takesue N, Fujii Y, Isobe M, Ueda Y, Sawa H, Kawada H, Murakami Y, David W I F and Ibberson R M 1998 *Physica* B **241–3** 534
[7] Loa I, Syassen K, Kremer R K, Schwarz U and Hanfland M 1999 *Phys. Rev.* B **60** R6945
[8] Loa I, Syassen K and Kremer R K 1999 *Solid State Commun.* **112** 681
[9] Loa I, Schwarz U, Hanfland M, Kremer R K and Syassen K 1999 *Phys. Status Solidi* b **215** 709
[10] Loa I, Grzechnik A, Schwarz U, Syassen K, Hanfland M and Kremer R K 2001 *J. Alloys Compounds* **317–18** 103
[11] Ohwada K, Fujii Y, Takesue N, Isobe M, Ueda Y, Nakao H, Wakabayashi Y, Murakami Y, Ito K, Amemiya Y, Fujihisa H, Aoki K, Noda Y and Ikeda N 2001 *Phys. Rev. Lett.* **87** 086402
[12] Huber G, Syassen K and Holzapfel W B 1977 *Phys. Rev.* B **15** 5123
[13] Konstantinović M J, Popović Z V, Isobe M and Ueda Y 2000 *Phys. Rev.* B **61** 15 185
[14] Popović Z V, Konstantinović M J, Gajić R, Popov V, Isobe M, Ueda Y and Moshchalkov V V 2002 *Phys. Rev.* B **65** 184303
[15] Popović Z V, Konstantinović M J, Gajić R, Popov V, Raptis Y S, Vasil'ev A N, Isobe M and Ueda Y 1999 *Solid State Commun.* **110** 381
[16] Onoda M and Nishiguchi N 1999 *J. Phys.: Condens. Matter* **11** 3475
[17] Clauws P, Broeckx J and Vennik J 1985 *Phys. Status Solidi* b **131** 459
[18] Grzechnik A 1998 *Chem. Mater.* **10** 2505
[19] Shen Z X, Ong C W, Tang S H and Kuok M H 1994 *J. Phys. Chem. Solids* **55** 661
Shen Z X, Ong C W, Tang S H and Kuok M H 1994 *J. Phys. Chem. Solids* **55** 665
Shen Z X, Ong C W, Tang S H and Kuok M H 1994 *Phys. Rev.* B **49** 1433